Excitation energies of dissociating H_2: A problematic case for the adiabatic approximation of time-dependent density functional theory

O. V. Gritsenko and S. J. A. van Gisbergen
Scheikundig Laboratorium der Vrije Universiteit, De Boelelaan 1083, 1081 HV Amsterdam, The Netherlands

A. Görling
Lehrstuhl für Theoretische Chemie, Technische Universität München, 85747 Garching, Germany

E. J. Baerends
Scheikundig Laboratorium der Vrije Universiteit, De Boelelaan 1083, 1081 HV Amsterdam, The Netherlands

(Received 5 June 2000; accepted 24 August 2000)

Time-dependent density functional theory (TDDFT) is applied for calculation of the excitation energies of the dissociating H_2 molecule. The standard TDDFT method of adiabatic local density approximation (ALDA) totally fails to reproduce the potential curve for the lowest excited singlet $^1\Sigma_u^+$ state of H_2. Analysis of the eigenvalue problem for the excitation energies as well as direct derivation of the exchange-correlation (xc) kernel $f_{\mathrm{xc}}(\mathbf{r},\mathbf{r}',\omega)$ shows that ALDA fails due to breakdown of its simple spatially local approximation for the kernel. The analysis indicates a complex structure of the function $f_{\mathrm{xc}}(\mathbf{r},\mathbf{r}',\omega)$, which is revealed in a different behavior of the various matrix elements $K^{\mathrm{xc}}_{1c,1c}$ (between the highest occupied Kohn–Sham molecular orbital ψ_1 and virtual MOs ψ_c) as a function of the bond distance R(H–H). The effect of nonlocality of $f_{\mathrm{xc}}(\mathbf{r},\mathbf{r}')$ is modeled by using different expressions for the corresponding matrix elements of different orbitals. Asymptotically corrected ALDA (ALDA-AC) expressions for the matrix elements $K^{\mathrm{xc}(\sigma\tau)}_{12,12}$ are proposed, while for other matrix elements the standard ALDA expressions are retained. This approach provides substantial improvement over the standard ALDA. In particular, the ALDA-AC curve for the lowest singlet excitation qualitatively reproduces the shape of the exact curve. It displays a minimum and approaches a relatively large positive energy at large R(H–H). ALDA-AC also produces a substantial improvement for the calculated lowest triplet excitation, which is known to suffer from the triplet instability problem of the restricted KS ground state. Failure of the ALDA for the excitation energies is related to the failure of the local density as well as generalized gradient approximations to reproduce correctly the polarizability of dissociating H_2. The expression for the response function χ is derived to show the origin of the field-counteracting term in the xc potential, which is lacking in the local density and generalized gradient approximations and which is required to obtain a correct polarizability. © *2000 American Institute of Physics.* [S0021-9606(00)31143-6]

I. INTRODUCTION

The recent success of time-dependent density functional perturbation theory (TDDFPT) in calculations of molecular excitation energies[1–7] is based on its efficient treatment of electron correlation. The effects of electron correlation in the stationary ground state are embodied in the single local Kohn–Sham (KS) exchange-correlation (xc) potential $\nu_{\mathrm{xc}}(\mathbf{r})$ which, together with the external potential $\nu_{\mathrm{ext}}(\mathbf{r})$ and the Hartree potential of the electrostatic electron repulsion $\nu_H(\mathbf{r})$, determines the KS orbitals ψ_i

$$\{-\tfrac{1}{2}\nabla^2+\nu_{\mathrm{ext}}(\mathbf{r})+\nu_H(\mathbf{r})+\nu_{\mathrm{xc}}(\mathbf{r})\}\psi_i(\mathbf{r})=\epsilon_i\psi_i(\mathbf{r}), \quad (1.1)$$

and the electron density $\rho(\mathbf{r})$ of a many-electron system

$$\rho(\mathbf{r})=\sum_{i=1}^{N}|\psi_i(\mathbf{r})|^2. \quad (1.2)$$

Excitation energies as well as polarizabilities are obtained in TDDFPT from the linear response of the density $\delta\rho(\mathbf{r},\omega)$ to the external electric field of frequency ω

$$\delta\rho(\mathbf{r},\omega)=\int d\mathbf{r}'\,\chi_s(\mathbf{r},\mathbf{r}',\omega)\Bigg\{\delta\nu_{\mathrm{ext}}(\mathbf{r}',\omega)+\int d\mathbf{r}''\frac{\delta\rho(\mathbf{r}'',\omega)}{|\mathbf{r}'-\mathbf{r}''|}+\delta\nu_{\mathrm{xc}}(\mathbf{r}',\omega)\Bigg\}, \quad (1.3)$$

where χ_s is the response function of the noninteracting KS system and the change of the xc potential is expressed through the xc kernel function $f_{\mathrm{xc}}(\mathbf{r},\mathbf{r}',\omega)$,

$$\delta\nu_{\mathrm{xc}}(\mathbf{r}',\omega)=\int d\mathbf{r}''\,\delta\rho(\mathbf{r}'',\omega)f_{\mathrm{xc}}(\mathbf{r}',\mathbf{r}'',\omega). \quad (1.4)$$

This function is defined in TDDFPT as the Fourier transform of the second functional derivative $f^{\sigma\tau}_{\mathrm{xc}}(\mathbf{r},\mathbf{r}',t,t')$ of the quantum mechanical action xc functional $A_{\mathrm{xc}}[\rho]$ with re-

spect to the time-dependent densities $\rho(\mathbf{r},t)$ and $\rho(\mathbf{r}',t')$,[8] for more refined definition see Ref. 9, for an alternative definition see Ref. 10 and Eq. (3.18):

$$f_{\mathrm{xc}}^{\sigma\tau}(\mathbf{r},\mathbf{r}',t,t')=\frac{\delta A_{\mathrm{xc}}[\rho]}{\delta\rho_{\sigma}(\mathbf{r},t)\,\delta\rho_{\tau}(\mathbf{r}',t)}=\frac{\delta\nu_{\mathrm{xc}}^{\sigma}([\rho];\mathbf{r},t)}{\delta\rho_{\tau}(\mathbf{r}',t)}. \tag{1.5}$$

The vertical excitation energies ω_k can be obtained in TDDFPT from the solution of the following eigenvalue problem:[11]

$$\begin{aligned}&[\bar{\varepsilon}^2+2\bar{\varepsilon}^{1/2}\mathbf{K}\bar{\varepsilon}^{1/2}]\mathbf{F}_k=\omega_k^2\mathbf{F}_k,\\&\bar{\varepsilon}_{ic\sigma,jd\tau}=(\varepsilon_{c\sigma}-\bar{\varepsilon}_{i\sigma})\,\delta_{\sigma\tau}\delta_{ij}\delta_{cd},\end{aligned} \tag{1.6}$$

where the matrix indices i and j correspond to the occupied KS orbitals, the indices c and d correspond to the unoccupied orbitals, and σ and τ are the spin indices (real orbitals are considered, we use indices c and d instead of the more common indices a and b as these are reserved for the atomic orbitals, which will be introduced below). The first term in the l.h.s. of Eq. (1.6), the orbital energy difference, represents the zero order of TDDFPT. The second term represents the correction, which is calculated with the coupling matrix $K_{ic\sigma,jd\tau}$[12]

$$\begin{aligned}K_{ic\sigma,jd\tau}=\int d\mathbf{r}\int d\mathbf{r}'\,\psi_{i\sigma}(\mathbf{r})\,\psi_{c\sigma}(\mathbf{r})\Bigg[&\frac{1}{|\mathbf{r}-\mathbf{r}'|}\\&+f_{\mathrm{xc}}^{\sigma\tau}(\mathbf{r},\mathbf{r}',\omega)\Bigg]\psi_{j\tau}(\mathbf{r}')\,\psi_{d\tau}(\mathbf{r}'),\end{aligned} \tag{1.7}$$

where the frequency dependence arises from the frequency dependent xc kernel $f_{\mathrm{xc}}(\mathbf{r},\mathbf{r}',\omega)$.

To our knowledge, in all molecular TDDFPT calculations the adiabatic approximation is used, which reduces f_{xc} to the time-(frequency-)independent second derivative of the ground state xc energy functional $E_{\mathrm{xc}}[\rho]$ or, equivalently, to the first derivative of the xc potential ν_{xc} of Eq. (1.1)

$$f_{\mathrm{xc}}^{\sigma\tau}(\mathbf{r},\mathbf{r}')\approx\frac{\delta E_{\mathrm{xc}}[\rho]}{\delta\rho_{\sigma}(\mathbf{r})\,\delta\rho_{\tau}(\mathbf{r}')}=\frac{\delta\nu_{\mathrm{xc}}^{\sigma}(\mathbf{r})}{\delta\rho_{\tau}(\mathbf{r}')}. \tag{1.8}$$

This seems to be a rather restrictive approximation for calculation of excitation energies, since with it all the excitations should be calculated from Eqs. (1.6), (1.7) with the same operators $|\mathbf{r}-\mathbf{r}'|^{-1}$ and $f_{\mathrm{xc}}(\mathbf{r},\mathbf{r}')$. In practice, however, already the zero order TDDFPT yields a decent estimate of excitations and, usually, reasonably good lowest excitation energies are obtained in the adiabatic local density approximation (ALDA) with the LDA xc potential $\nu_{\mathrm{xc}}^{\sigma(\mathrm{LDA})}$ and the ALDA xc kernel

$$f_{\mathrm{xc}}^{\sigma\tau(\mathrm{ALDA})}(\mathbf{r},\mathbf{r}')=\delta(\mathbf{r}-\mathbf{r}')\left.\frac{d\,\nu_{\mathrm{xc}}^{\sigma(\mathrm{LDA})}}{d\rho_{\tau}}\right|_{\rho_{\tau}=\rho_{\tau(\mathrm{SCF})}}. \tag{1.9}$$

As was found in Ref. 13 for atomic systems (and small molecular systems), further significant improvement of the results can be achieved, when an essentially accurate ν_{xc} constructed from the *ab initio* density ρ is combined with the $f_{\mathrm{xc}}^{\sigma\tau(\mathrm{ALDA})}$ of Eq. (1.9). To improve the quality of approximate ν_{xc}, specialized asymptotic corrections have been grafted onto the LDA potential[14] and the xc potential of the generalized gradient approximation (GGA),[15] while in Ref. 16 an approximate orbital-dependent ν_{xc} employing a statistical average of different model orbital potentials (SAOP)[17] has been developed. Combined with $f_{\mathrm{xc}}^{\sigma\tau(\mathrm{ALDA})}$, these model potentials have produced considerable improvement of the calculated excitation energies for some small molecules.[14–16] Thus the conclusion has been drawn that, at least for small molecules at their equilibrium geometry, the frequency dependence of the xc kernel is not important and reliable excitation energies can be obtained with a combination of the simple frequency-independent ALDA kernel Eq. (1.9) and a properly modeled potential ν_{xc}.

This conclusion promises a bright future for TDDFPT applications to molecular excitation energies and related properties, such as (hyper)polarizabilities, as it is reasonable to expect further improvements in the modeling of the xc potential in the near future. Indeed, TDDFPT has not only been successfully applied to the excitation energies of small molecules, but also (and perhaps more important) to such diverse systems as (higher) fullerenes,[18,19] (metal-containing) porphyrin-based systems,[20–22] transition metal complexes.[23,24] In all of these cases the TDDFPT results belong to the highest level results available. We believe that the ALDA is a minor source of errors in those applications, as it is for the small molecules.

However, there are cases where TDDFPT calculations are not so accurate. It has been shown in Refs. 25–27 that LDA/ALDA calculations strongly overestimate the (hyper) polarizabilities of both symmetric and asymmetric (terminated with strong donor and acceptor groups) conjugated molecular chains. This problem is related to an increasing underestimation of excitation energies in such systems[28,29] and has been analyzed in detail in Refs. 30, 31. It has been shown that the LDA xc potential of a molecular chain in a finite electric field misses a linear term, which counteracts the applied electric field. Such a term is present in the exact xc potential and in the Krieger–Li–Iafrate (KLI)[32] exchange-only potential. In a TDDFPT calculation the counteracting term should be present in $\delta\nu_{\mathrm{xc}}$ and the lack of it indicates a deficiency of f_{xc}, cf. Eq. (1.4).

Another important case where the use of the popular ALDA xc kernel Eq. (1.9) drastically fails is the dissociating H_2 molecule. It is already known[30,31] that LDA/ALDA calculations strongly overestimate the polarizability in finite field calculations on this system due to the lack of the term in $\delta\nu_{\mathrm{xc}}$, which counteracts $\delta\nu_{\mathrm{ex}}$. Analysis of this problem in terms of the conditional probability amplitudes performed in Ref. 31 reveals that the field-counteracting term of $\delta\nu_{\mathrm{xc}}$ represents the effect of the nondynamical (left–right) Coulomb correlation. When using the linear response approach of Eq. (1.3) to calculate the polarizability, it is clear from Eq. (1.4) that this term has to be generated with the correlation component of f_{xc} having proper magnitude and spatial form.

In the present paper we will focus on the problems with the TDDFPT calculation of the excitation energies and excited state potential energy curves of the dissociating H_2 molecule. We will address specifically the error for the first excited singlet state, which is particularly large and which is

related to the strong overestimation of the polarizability mentioned above. We will include in our discussion the triplet state, which has been considered before[33,34] (see for a discussion of the analogous TDHF case Ref. 35). The problems with the excitation energies are of great importance because of possible applications of TDDFPT in photochemistry, where the excited state energies are needed for various separations between the products of the photochemical reaction. The potential energy surfaces of molecular excited states can be calculated by collecting for a certain excited state k the corresponding vertical excitations $\omega_k(\mathbf{R}) = E_k(\mathbf{R}) - E_0(\mathbf{R})$ calculated with TDDFPT at various geometries $\{\mathbf{R}\}$. In this way, one can produce the differential potential energy surface of the state k with respect to the ground state. Then, adding the total ground state energy $E_0(\mathbf{R})$ calculated within the standard density functional theory (DFT), one can obtain the total potential energy surface $E_k(\mathbf{R})$ of this state, provided the ground state potential curve is of good quality. Potential energy curves obtained with this technique have been reported recently.[14,36]

In this paper TDDFPT is applied to calculation of the differential potential energy curves of the lowest excited singlet and triplet states of Σ_u symmetry of the H_2 molecule. Comparison of the exact[37,38] and ALDA potential energy curves in Sec. II shows that at larger R(H–H) ALDA fails to reproduce even qualitatively the shape of the potential curves for the $^3\Sigma_u^+$ and $^1\Sigma_u^+$ states. In this case the zero order TDDFPT, the difference $\Delta\epsilon_{21}$ between the energies of the lowest unoccupied (LUMO) ψ_2, and highest occupied (HOMO) ψ_1 Kohn–Sham orbitals of H_2 give a poor estimate of the lowest singlet–singlet excitation, vanishing with R(H–H). In Sec. III the electron response and excitations in dissociating H_2 are analyzed within the minimal two-orbital model, in which only $1s$ atomic orbitals (AOs) of H atoms are taken into account. An analysis of the rigorous TDDFT eigenvalue equations shows, that for the lowest singlet–singlet excitation ω_{s1} the correct matrix element $K_{12,12}^{\mathrm{xc}}$ of f_{xc} between HOMOψ_1 and LUMOψ_2 is positive and diverges with increasing bond length proportionally to the inverse HOMO-LUMO gap $(\Delta\varepsilon_{21})^{-1}$. In Sec. IV this feature is taken into account by means of an asymptotic correction to the matrix element $K_{12,12}^{\mathrm{xc(ALDA)}}$. The corresponding asymptotically corrected ALDA (ALDA-AC) provides a substantial improvement over the standard ALDA. In particular, the ALDA-AC curve for the lowest singlet excitation qualitatively reproduces the main features of the exact curve. In Sec. V an extended model with the Heitler–London wave functions built from $1s,2s,2p\sigma$ AOs is applied to obtain a direct estimate of the interacting response function χ, the noninteracting χ_s, and the xc kernel $f_{\mathrm{xc}}(\mathbf{r},\mathbf{r}',\omega)$. The response function χ of the extended model affords a realistic polarizability of dissociating H_2, which properly approaches the polarizabilities of two isolated H atoms. The derived expression for the response function χ is also used in Sec. V to show the origin of the field-counteracting term in the xc potential, which is required in order to reproduce correctly within TDDFT the polarizability of dissociating H_2. This establishes the connection between the current problem of excitation energies with TDDFT in the adiabatic local density approximation and the failure of DFT response theory for (hyper)polarizabilities of linear chains.[30,31] The behavior of $f_{\mathrm{xc}}(\mathbf{r},\mathbf{r}',\omega)$ is much harder to derive in the more realistic extended orbital model than in the minimal model, but an adiabatic approximation (ω-independent f_{xc}) should still be possible with such a spatial structure of f_{xc} that the $K_{12,12}$ matrix element diverges but not the other K-matrix elements. In Sec. VI the implications of these results for TDDFPT are discussed and the conclusions are drawn.

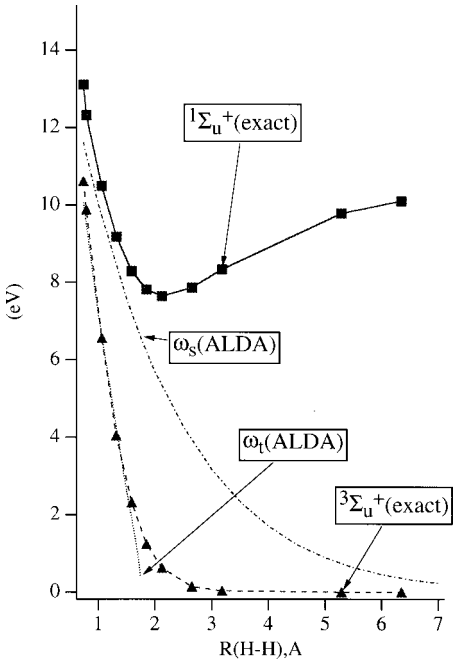

FIG. 1. Comparison of the exact and ALDA differential potential curves for H_2.

II. COMPARISON OF THE ALDA AND EXACT POTENTIAL CURVES

Figure 1 compares the exact excitation energies $[E(^3\Sigma_u^+) - E(^1\Sigma_g^+)]$ and $[E(a^1\Sigma_u^+) - E(^1\Sigma_g^+)]$ for the lowest $^3\Sigma_u^+$ and $^1\Sigma_u^+$ states of H_2 with the lowest triplet and singlet ALDA excitation energies ω_{t1}, ω_{s1}. The exact curves have been produced from the benchmark data of Refs. 36, 37, while the energies ω_{t1} and ω_{s1} are obtained from Eqs. (1.6) with the LDA xc potential $\nu_{\mathrm{xc}}^{\sigma(\mathrm{LDA})}(\mathbf{r})$ and the ALDA xc kernel Eq. (1.9). The ALDA calculations have been performed in the triple-zeta basis set of the Slater-type orbitals (STO) augmented with two polarization functions and one *s*, *p*, and *d* diffuse function per each H atom. Although this is a reliable basis set, we have made no attempt of obtaining results very close to the basis set limit.

The exact excitation energies $[E(^3\Sigma_u^+) - E(^1\Sigma_g^+)]$ and $[E(^1\Sigma_u^+) - E(^1\Sigma_g^+)]$ differ very much in their dependence on the interatomic distance R(H–H): the triplet excitation energy decreases monotonically with increasing R(H–H) and it vanishes in the limit $R(\mathrm{H–H}) \to \infty$. Contrary to this, the singlet excitation energy increases beyond the equilibrium distance for the stable $^1\Sigma_u^+$ state and it approaches 10.2 eV for $R(\mathrm{H–H}) \to \infty$. This indicates a different nature of the states $^3\Sigma_u^+$ and $^1\Sigma_u^+$. The former state, as well as the ground

state $^1\Sigma_g^+$, is of covalent type, i.e., they both represent the two electrons of H_2 located instantaneously on the $1s$AOs of different H atoms. Whether these electrons are of the same spin (as in the $^3\Sigma_u^+$ state), or of opposite spin (as in the $^1\Sigma_g^+$ state) makes less difference with increasing R(H–H). Because of this, the differential potential energy curve $E(^3\Sigma_u^+)-E(^1\Sigma_g^+)$ gradually approaches zero at larger R(H–H) (see Fig. 1). Contrary to this, the $^1\Sigma_u^+$ state is represented by a combination of the ionic state, which eventually dissociates to H^+ and H^- and the ''promoted'' states, which dissociate to one normal H atom and one excited atom H* (in H* the electron is promoted to the $2s$ or $2p_\sigma$ AO). At distances R(H–H)<3.7 Å the ionic component prevails, while at larger R(H–H), due to the avoided crossing of the potential curves, the ''promoted'' states bring a dominant contribution. Due to this, the corresponding exact curve approaches the value of 10.2 eV, which is just the atomic energy of $1s\rightarrow 2s$ or $2p_\sigma$ promotion.

We proceed with the comparison of the exact and ALDA potential curves. For shorter R(H–H) around 1 Å the ALDA triplet ω_{t1} and singlet ω_{s1} excitation energies are rather close to the exact ones. However, for larger R(H–H) the ALDA curves have a very different form compared to the exact ones. In particular, the ALDA curve for the triplet excitation suffers from the triplet instability problem.[38] It reaches the zero value at the triplet instability point at R(H–H) $=1.75$ Å, beyond which the solution of the TDDFPT eigenvalue problem Eq. (1.6) yields an unphysical negative value of ω^2 for this state. And, in a complete disagreement with the exact theory ALDA predicts a small lowest singlet excitation energy for the dissociating H_2, since the calculated ω_{s1} value gradually approaches zero at larger R(H–H). Furthermore, the corresponding ALDA solution of the eigenvalue problem Eq. (1.6) does not exhibit the characteristic features of the avoided crossing of potential curves, which was mentioned above for the exact curves. As follows from the analysis of the calculated weights of the single-particle transitions, ALDA describes the lowest singlet excitation as a nearly pure transition from the HOMO$\psi_1(\mathbf{r})$

$$\psi_1(\mathbf{r})=1\sigma_g(\mathbf{r})=\frac{1}{\sqrt{2+2S_1}}[a_1(\mathbf{r})+b_1(\mathbf{r})], \tag{2.1}$$

to the LUMO $\psi_2(\mathbf{r})$

$$\psi_2(\mathbf{r})=1\sigma_u(\mathbf{r})=\frac{1}{\sqrt{2-2S_1}}[a_1(\mathbf{r})-b_1(\mathbf{r})]. \tag{2.2}$$

Both orbitals consist almost purely of $1s$ AOs $a_1(\mathbf{r})$ and $b_1(\mathbf{r})$ located on atoms H_A and H_B, respectively, so that the ALDA solution exhibits no admixture of $2s$,$2p$ AOs, the latter being the characteristic feature of the avoided crossing of potential curves.

In order to gain some insight into this failure of ALDA, Fig. 2 compares the exact potential curves with the HOMO-LUMO gap $\Delta\varepsilon_{21}$ which, according to Eq. (1.6), is the ALDA zero order estimate for both singlet ω_{s1} and triplet ω_{t1} excitation energies. The $\Delta\varepsilon_{21}$ curve resembles the exact excitation energy for the triplet excitation, $\Delta\varepsilon_{21}$ also vanishes with R(H–H), although more slowly than the difference

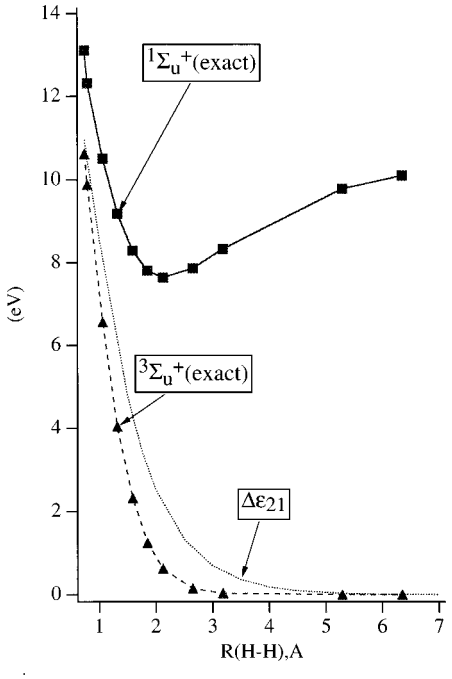

FIG. 2. Comparison of the exact differential potential curves with the KS HOMO-LUMO energy difference for H_2.

$[E(^3\Sigma_u^+)-E(^1\Sigma_g^+)]$, so that $[E(^3\Sigma_u^+)-E(^1\Sigma_g^+)]/\Delta\varepsilon_{21}\ll 1$ at large R(H–H). Thus $\Delta\varepsilon_{21}$ can be considered as an acceptable zero order estimate of the exact triplet excitation energy $[E(^3\Sigma_u^+)-E(^1\Sigma_g^+)]$, i.e., the correction to the zero order from the coupling matrix Eq. (1.7), which is needed in order to reproduce the exact triplet curve, should be relatively small. Contrary to this, the zero order ALDA provides a very poor estimate for the lowest singlet excitation, i.e. the analogous correction to $\Delta\varepsilon_{21}$ to reproduce the exact $[E(^1\Sigma_u^+)-E(^1\Sigma_g^+)]$ curve should be positive and large for R(H–H) >2 Å (see Fig. 2). Clearly, taken together in Eq. (1.7) with the Coulomb term, the simple ALDA approximation Eq. (1.9) for f_{xc} cannot provide such a correction. This causes the abovementioned failure of ALDA for the lowest singlet excitation, which is illustrated in Fig. 1. In the next sections the cause of the ALDA failure as well as the features the correct xc kernel should possess to remedy this failure will be analyzed.

III. A MINIMAL TWO-ORBITAL 1*s*-MODEL

A minimal two-orbital model of dissociating H_2 considers only $1s$ AOs $a_1(\mathbf{r})$ and $b_1(\mathbf{r})$ located on atoms H_A and H_B, respectively. With these orbitals, a qualitative description of the electronic structure of the ground $^1\Sigma_g^+$ and the excited $^3\Sigma_u^+$, $^1\Sigma_u^+$, $^1\Sigma_g^+$ can be given with the corresponding Heitler–London (HL) wave functions, which become more accurate for larger R(H–H)

$$\Psi_0^{HL}(^1\Sigma_g^+)=\frac{1}{2(1+S_1^2)^{1/2}}[a_1(\mathbf{r}_1)b_1(\mathbf{r}_2)+b_1(\mathbf{r}_1)a_1(\mathbf{r}_2)] \times[\alpha(1)\beta(2)-\beta(1)\alpha(2)], \tag{3.1}$$

$$\Psi_1^{HL}(^3\Sigma_u^+)=\frac{1}{2^{1/2}(1-S_1^2)^{1/2}}[a_1(\mathbf{r}_1)b_1(\mathbf{r}_2)-b_1(\mathbf{r}_1)a_1(\mathbf{r}_2)] \times\begin{cases}[\alpha(1)\beta(2)+\beta(1)\alpha(2)]/2^{1/2}, & M_s=0\\ \alpha(1)\alpha(2), & M_s=1\\ \beta(1)\beta(2), & M_s=-1\end{cases}, \tag{3.2}$$

$$\Psi_2^{HL}(^1\Sigma_u^+)=\frac{1}{2(1-S_1^2)^{1/2}}[a_1(\mathbf{r}_1)a_1(\mathbf{r}_2)-b_1(\mathbf{r}_1)b_1(\mathbf{r}_2)] \times[\alpha(1)\beta(2)-\beta(1)\alpha(2)], \tag{3.3}$$

$$\Psi_3^{HL}(^1\Sigma_g^+)=\left\{\frac{(1+S_1^2)^{1/2}}{2(1+S_1^2)}[a_1(\mathbf{r}_1)a_1(\mathbf{r}_2)+b_1(\mathbf{r}_1)b_1(\mathbf{r}_2)] -\frac{S_1}{(1+S_1^2)^{1/2}(1-S_1^2)}[a_1(\mathbf{r}_1)b_1(\mathbf{r}_2) +b_1(\mathbf{r}_1)a_1(\mathbf{r}_2)]\right\}[\alpha(1)\beta(2)-\beta(1)\alpha(2)]. \tag{3.4}$$

In Eqs. (3.1)–(3.4) α and β are the spin functions and S_1 is the overlap integral between $a_1(\mathbf{r})$ and $b_1(\mathbf{r})$. The function $\Psi_3^{HL}(^1\Sigma_g^+)$ is properly orthogonalized to $\Psi_0^{HL}(^1\Sigma_u^+)$. It is well known that the covalent wave function $\Psi_0^{HL}(^1\Sigma_u^+)$ becomes a better description of the ground state at long bond distances, while closer to the equilibrium bond length the ionic wave function [the first term of $\Psi_3^{HL}(^1\Sigma_g^+)$] mixes into the ground state. In the context of this paper it is important to note, from Eqs. (3.2)–(3.3), the covalent nature of the excited state $\Psi_1^{HL}(^3\Sigma_u^+)$ and the ionic nature of the state $\Psi_2^{HL}(^1\Sigma_u^+)$. Indeed, the spatial part of the wave function Eq. (3.2) represents a covalent situation with the two electrons of H_2 located on the $1s$ AOs of different H atoms, while that of the wave function Eq. (3.3) [and indeed the first term of Eq. (3.4)] represents an ionic picture with both electrons instantaneously located on the same H atom.

Within the KS theory, we are dealing with an independent particle picture with—usually—a single determinantal wave function. The KS determinant need not be a good approximation to the true ground state wave function. In dissociating H_2 the KS ground state is represented with the determinant $\Psi_s=|\psi_1^{(\uparrow)}(1)\psi_1^{(\downarrow)}(2)|$, where ψ_1 is the HOMO Eq. (2.1). This holds even at very long bond distances, where the KS determinant becomes an equal mixture of the covalent and ionic Heitler–London functions Eqs. (3.1) and (3.4), whereas the true ground state wave function is the covalent Heitler–London wave function. As a matter of fact, the KS orbital ψ_1 differs at the bond midpoint from the simple combination of the $1s$ atomic orbitals Eq. (2.1). This reflects the fact that in the exact wave function the doubly excited configuration ψ_2^2 mixes strongly into the Hartree–Fock configuration ψ_1^2, modifying the density at the bond midpoint where ψ_2 has a node. We refer to Ref. 39 for an analysis of the behavior of the KS orbital of dissociating H_2 around the bond midpoint; for the present paper this subtle point is unimportant.

We proceed with the analysis of the rigorous eigenvalue equations (1.6) for excitation energies of H_2. Within the spin-restricted TDDFPT, the only legitimate approach for the closed-shell H_2 molecule, triplet and singlet excitation energies are obtained separately from the solution of the following eigenvalue equations

$$\Omega^S_{ic,jd}\mathbf{F}_k=\omega_k^2\mathbf{F}_k, \tag{3.5}$$

$$\Omega^T_{ic,jd}\mathbf{F}_k=\omega_k^2\mathbf{F}_k, \tag{3.6}$$

$$\Omega^S_{ic,jd}=\delta_{ij}\delta_{cd}(\varepsilon_c-\varepsilon_i)^2+2\sqrt{(\varepsilon_c-\varepsilon_i)}[2K^{\mathrm{Coul}}_{ic,jd} +K^{\mathrm{xc}}_{ic,jd}(\omega)]\sqrt{(\varepsilon_d-\varepsilon_j)}, \tag{3.7}$$

$$K^{\mathrm{xc}}_{ic,jd}(\omega)=K^{\mathrm{xc}\uparrow\uparrow}_{ic,jd}(\omega)+K^{\mathrm{xc}(\uparrow\downarrow)}_{ic,jd}(\omega), \tag{3.8}$$

$$\Omega^T_{ic,jd}=\delta_{ij}\delta_{cd}(\varepsilon_c-\varepsilon_i)^2+2\sqrt{(\varepsilon_c-\varepsilon_i)}[K^{\mathrm{xc}(\uparrow\uparrow)}_{ic,jd}(\omega) -K^{\mathrm{xc}(\uparrow\downarrow)}_{ic,jd}(\omega)]\sqrt{(\varepsilon_d-\varepsilon_j)}. \tag{3.9}$$

In Eqs. (3.7)–(3.9) the coupling matrix is split into the Coulomb part

$$K^{\mathrm{Coul}}_{ic,jd}=\int d\mathbf{r}\int d\mathbf{r}'\,\psi_i(\mathbf{r})\psi_c(\mathbf{r})\frac{1}{|\mathbf{r}-\mathbf{r}'|}\psi_j(\mathbf{r}')\psi_d(\mathbf{r}'), \tag{3.10}$$

and the xc parts

$$K^{\mathrm{xc}(\uparrow\uparrow)}_{ic,jd}(\omega)=\int d\mathbf{r}\int d\mathbf{r}'\,\psi_i(\mathbf{r})\psi_c(\mathbf{r})f_{\mathrm{xc}}^{(\uparrow\uparrow)} \times(\mathbf{r},\mathbf{r}',\omega)\psi_j(\mathbf{r}')\psi_d(\mathbf{r}'), \tag{3.11}$$

$$K^{\mathrm{xc}(\uparrow\downarrow)}_{ic,jd}(\omega)=\int d\mathbf{r}\int d\mathbf{r}'\,\psi_i(\mathbf{r})\psi_c(\mathbf{r})f_{\mathrm{xc}}^{(\uparrow\downarrow)} \times(\mathbf{r},\mathbf{r}',\omega)\psi_j(\mathbf{r}')\psi_d(\mathbf{r}'), \tag{3.12}$$

In the present minimal two-orbital model the rigorous matrix Eqs. (3.7), (3.9) reduce to the straightforward formulas for the excitation energies ω_{s1} and ω_{t1}

$$\omega_{s1}=\sqrt{\Delta\varepsilon_{21}[\Delta\varepsilon_{21}+4K^{\mathrm{Coul}}_{12,12}+2(K^{\mathrm{xc}(\uparrow\uparrow)}_{12,12}(\omega=\omega_{s1})+K^{\mathrm{xc}(\uparrow\downarrow)}_{12,12}(\omega=\omega_{s1}))]}, \tag{3.13}$$

$$\omega_{t1}=\sqrt{\Delta\varepsilon_{21}[\Delta\varepsilon_{21}+2(K^{\mathrm{xc}(\uparrow\uparrow)}_{12,12}(\omega=\omega_{t1})-K^{\mathrm{xc}(\uparrow\downarrow)}_{12,12}(\omega=\omega_{t1}))]}, \tag{3.14}$$

where the matrix elements $K_{12,12}$ are calculated with the orbitals ψ_1 and ψ_2. First, we consider the expression Eq. (3.13) for the lowest singlet excitation ω_{s1}. For larger R(H–H) the orbital energy difference $\Delta\varepsilon_{21}$ approaches zero and the Coulomb integral $K_{12,12}^{\mathrm{Coul}}$ remains finite (it reduces to twice a local atomic contribution), so that, after multiplication by $\Delta\varepsilon_{21}$, we can neglect the first two terms under the square root of Eq. (3.13),

$$\omega_{s1}=\sqrt{2\Delta\varepsilon_{21}(K_{12,12}^{\mathrm{xc}(\uparrow\uparrow)}(\omega=\omega_{s1})+K_{12,12}^{\mathrm{xc}(\uparrow\downarrow)}(\omega=\omega_{s1}))}. \tag{3.15}$$

However, as was indicated in the previous section, the exact singlet excitation energy $\omega(^1\Sigma_g^+\rightarrow{}^1\Sigma_u^+)$ remains finite (and large) at large R(H–H). From this and Eq. (3.15) follows that the sum of the matrix elements $(K_{12,12}^{\mathrm{xc}(\uparrow\uparrow)}(\omega=\omega_{s1})+K_{12,12}^{\mathrm{xc}(\uparrow\downarrow)}(\omega=\omega_{s1}))$ should be positive and it should diverge as $(\Delta\varepsilon_{21})^{-1}$ with increasing R(H–H):

$$K_{12,12}^{\mathrm{xc}(\uparrow\uparrow)}(\omega=\omega_{s1})+K_{12,12}^{\mathrm{xc}(\uparrow\downarrow)}(\omega=\omega_{s1}) \sim\frac{1}{\Delta\varepsilon_{21}},\ \text{at large}\ R(\text{H–H}). \tag{3.16}$$

Contrary to this, the exact triplet excitation energy $\omega(^1\Sigma_g^+\rightarrow{}^3\Sigma_u^+)$ approaches zero at large R(H–H) with $\omega(^1\Sigma_g^+\rightarrow{}^3\Sigma_u^+)\ll\Delta\varepsilon_{12}$. From this and Eq. (3.14) follows that the difference $[K_{12,12}^{\mathrm{xc}(\uparrow\uparrow)}(\omega=\omega_{t1})\text{-}K_{12,12}^{\mathrm{xc}(\uparrow\downarrow)}(\omega=\omega_{t1})]$ should be negative and it should approach $-\Delta\varepsilon_{21}/2$ from above

$$[K_{12,12}^{\mathrm{xc}(\uparrow\uparrow)}(\omega=\omega_{t1})-K_{12,12}^{\mathrm{xc}(\uparrow\downarrow)}(\omega=\omega_{t1})] \rightarrow-\Delta\varepsilon_{21}/2+0,\ \text{at large}\ R(\text{H–H}). \tag{3.17}$$

Since the exact xc functions $K_{12,12}^{\mathrm{xc}(\uparrow\uparrow)}$ and $K_{12,12}^{\mathrm{xc}(\uparrow\downarrow)}$ are not known, we can analyze various variants satisfying Eqs. (3.16), (3.17). One option is a strong frequency dependence of the function $K_{12,12}^{\mathrm{xc}(\uparrow\downarrow)}(\omega)$. It can diverge as $(\Delta\varepsilon_{21})^{-1}$ at the frequency $\omega=\omega_{s1}$, while it remains finite and close to $K_{12,12}^{\mathrm{xc}(\uparrow\uparrow)}(\omega=\omega_{t1})$ at $\omega=\omega_{t1}$. With a finite $K_{12,12}^{\mathrm{xc}(\uparrow\uparrow)}(\omega)$ at all frequencies, this can satisfy Eqs. (3.16), (3.17). Another option is that both $K_{12,12}^{\mathrm{xc}(\uparrow\uparrow)}$ and $K_{12,12}^{\mathrm{xc}(\uparrow\downarrow)}$ are approximately frequency-independent and diverge as $(\Delta\varepsilon_{21})^{-1}$. Then, their sum $[K_{12,12}^{\mathrm{xc}(\uparrow\uparrow)}+K_{12,12}^{\mathrm{xc}(\uparrow\downarrow)}]$ produces the required divergence, cf. Eq. (3.16), while their difference $[K_{12,12}^{\mathrm{xc}(\uparrow\uparrow)}-K_{12,12}^{\mathrm{xc}(\uparrow\downarrow)}]$ in Eq. (3.17) could vanish as $-\Delta\varepsilon_{21}/2$. One can get further insight into the form of the xc kernel $f_{\mathrm{xc}}(\omega)$ using its expression in terms of the difference between the inverse χ_s^{-1} of the KS noninteracting response function and the inverse χ^{-1} of the interacting response function[8]

$$f_{\mathrm{xc}}(\mathbf{r},\mathbf{r}',\omega)=\chi_x^{-1}(\mathbf{r},\mathbf{r}',\omega)-\chi^{-1}(\mathbf{r},\mathbf{r}',\omega)-\frac{1}{|\mathbf{r}-\mathbf{r}'|}. \tag{3.18}$$

The expression Eq. (3.18) is an alternative definition to Eq. (1.5) of f_{xc}. In the present minimal model the noninteracting response function χ_s, which enters Eqs. (1.3) and (3.18), consists of just one term

$$\chi_s(\mathbf{r},\mathbf{r}',\omega)=\frac{4\Delta\varepsilon_{21}}{\omega^2-\Delta\varepsilon_{21}^2}\psi_1(\mathbf{r})\psi_2(\mathbf{r})\psi_2(\mathbf{r}')\psi_1(\mathbf{r}'). \tag{3.19}$$

From Eq. (3.19) follows that the KS response function $\chi_s(\omega)$ of dissociating H_2 diverges as $-(\Delta\varepsilon_{21})^{-1}$ at small frequencies $|\omega|<\Delta\varepsilon_{21}$. In the static limit $\omega\rightarrow0$ this divergence leads according to Eq. (1.3) to a much too large uncoupled polarizability [neglecting the induced Hartree and xc potentials in Eq. (1.3)]. As a matter of fact, special behavior of δv_{xc} must prevent such unphysical large polarizability. It can indeed be shown that in dissociating H_2 $\delta\nu_{\mathrm{xc}}$ will exhibit a step behavior in going from the high-field to the low-field H atom, which counteracts the applied field. It has been noted in Ref. 30 that this behavior is analogous to the counteracting field that has to be produced by $\delta\nu_{\mathrm{xc}}$ in calculations on linear chains in a polarizing field.[40] Of course, the far too low singlet excitation energy, related to $\Delta\varepsilon_{21}$ going to 0, is related to the overestimation of the LDA and GGA polarizability and the counteracting potential problem. The ionic situation, in state $^1\Sigma_u^+$, corresponding to a highly polarized system, should not be so easily accessible, i.e., should be at much higher energy. We return to this problem in Sec. V.

At larger frequencies $|\omega|>\Delta\varepsilon_{21}$ the function $\chi_s(\omega)$ vanishes as $\Delta\varepsilon_{21}$. From the established behavior of $\chi_s(\omega)$ follows that its inverse $\chi_s^{-1}(\omega)$ vanishes at small frequencies $|\omega|<\Delta\varepsilon_{21}$ and $\chi_s^{-1}(\omega)$ diverges at $|\omega|>\Delta\varepsilon_{21}$.

The interacting response function χ can be calculated straightforwardly with the ground and excited state Heitler–London wave functions Eqs. (3.1), (3.3), (3.4) and the corresponding energies from the following expression for the density–density response function

$$\chi(\mathbf{r},\mathbf{r}',\omega)=\sum_j\frac{2[E_j-E_0]}{\omega^2-[E_j-E_0]^2}\langle\Psi_0^{HL}|\hat{\rho}(\mathbf{r})|\Psi_j^{HL}\rangle \times\langle\Psi_j^{HL}|\hat{\rho}(\mathbf{r}')|\Psi_0^{HL}\rangle, \tag{3.20}$$

where $\hat{\rho}(\mathbf{r})=\Sigma_{i=1}^N\delta(\mathbf{r}_i-\mathbf{r})$. Only singlet states contribute to the sum Eq. (3.20) and in the minimal model these are the states Ψ_2^{HL} of Eq. (3.3) and Ψ_3^{HL} of Eq. (3.4). Inserting Eqs. (3.3) and (3.4) in Eq. (3.20), and performing the required integrations, we obtain the following explicit expression for the interacting response function

$$\begin{aligned}\chi(\mathbf{r},\mathbf{r}',\omega)\approx{}&\frac{2(E_2-E_0)}{[\omega^2-(E_2-E_0)^2]}\frac{S_1^2}{(1-S_1^2)^2}[a_1^2(\mathbf{r})-b_1^2(\mathbf{r})]\\&\times[a_1^2(\mathbf{r}')-b_1^2(\mathbf{r}')]+\frac{2(E_3-E_0)}{[\omega^2-(E_3-E_0)^2]}\\&\times\frac{[-S_1a_1^2(\mathbf{r})-S_1b_1^2(\mathbf{r})+2a_1(\mathbf{r})b_1(\mathbf{r})]}{(1+S_1^2)}\\&\times\frac{[-S_1a_1^2(\mathbf{r}')-S_1b_1^2(\mathbf{r}')+2a_1(\mathbf{r}')b_1(\mathbf{r}')]}{(1+S_1^2)}.\end{aligned} \tag{3.21}$$

Note that both terms in Eq. (3.21) are proportional to the square S_1^2 of the atomic orbital overlap [for the second term we can consider the products $a(\mathbf{r})b(\mathbf{r})$ and $a(\mathbf{r}')b(\mathbf{r}')$ in the numerator proportional to S_1]. Thus for all but the resonance frequencies $\chi(\mathbf{r},\mathbf{r}',\omega)$ of Eq. (3.21) vanishes as S_1^2 with the bond length R(H–H); this is true, in particular, for the static response function $\chi(\mathbf{r},\mathbf{r}',0)$. From this it follows that the inverse response function $\chi^{-1}(\mathbf{r},\mathbf{r}',\omega)$ diverges as S_1^{-2}.

With the established behavior of $\chi_s^{-1}(\omega)$ and $\chi^{-1}(\omega)$, one can estimate the behavior of the xc kernel $f_{xc}(\omega)$ from the relation Eq. (3.18). In particular, at small frequencies $|\omega|<\Delta\varepsilon_{21}$ the function $f_{xc}(\omega)$ diverges, since the interacting function $\chi^{-1}(\omega)$ diverges, while the noninteracting $\chi_s^{-1}(\omega)$ vanishes at these frequencies. At frequencies $|\omega|>\Delta\varepsilon_{21}$ both $\chi_s^{-1}(\omega)$ and $\chi^{-1}(\omega)$ diverge. Still, the corresponding response functions Eqs. (3.19) and (3.21) are not identical to each other, so that one can assume that the divergencies of $\chi_s^{-1}(\omega)$ and $\chi^{-1}(\omega)$ would not cancel each other and, as a result, the $f_{xc}(\omega)$ will also diverge at these frequencies. Thus from this analysis it follows, that in the minimal model the xc kernel $f_{xc}(\omega)$ diverges with R(H–H). This result is consistent with the divergence Eq. (3.16) of the corresponding matrix element $K_{12,12}^{xc}=(K_{12,12}^{xc(\uparrow\uparrow)}+K_{12,12}^{xc(\uparrow\downarrow)})$, which has been found from the analysis of the eigenvalue problem. In the next section a model asymptotic correction to the ALDA xc kernel will be proposed, which recovers this divergence.

In the end of this section we would like to point out the limitations of the minimal model. To illustrate these limitations, we insert the interacting response function Eq. (3.21) of the minimal model in the expression for the static density response $\delta\rho(\mathbf{r},0)$ to the external field $\delta\nu_{ext}(\mathbf{r})$

$$\delta\rho(\mathbf{r},0)=\int d\mathbf{r}'\,\chi(\mathbf{r},\mathbf{r}',0)\,\delta\nu_{ext}(\mathbf{r}'). \tag{3.22}$$

We assume a field $\delta\nu_{ext}(\mathbf{r})=Ez$, where z is the molecular axis, so that H_A is the down-field atom and H_B is the up-field one. In this case the second term of Eq. (3.21) has zero contribution to Eq. (3.22) due to the symmetry and $\delta\rho$ is defined with the following expression

$$\delta\rho(\mathbf{r},0)=\frac{2}{-(E_2-E_0)}\frac{S_1^2}{(1-S_1^2)^2}[a_1^2(\mathbf{r})-b_1^2(\mathbf{r})] \times(\overline{\delta\nu_{A1}}-\overline{\delta\nu_{B1}}), \tag{3.23}$$

where $\overline{\delta\nu_{A1}}$ and $\overline{\delta\nu_{B1}}$ are the one-center field integrals $\overline{\delta\nu_{A1}}=\int d\mathbf{r}a_1^2(\mathbf{r})\,\delta\nu_{ext}(\mathbf{r})$, $\overline{\delta\nu_{B1}}=\int d\mathbf{r}b_1^2(\mathbf{r})\,\delta\nu_{ext}(\mathbf{r})$ with $\overline{\delta\nu_{A1}}<\overline{\delta\nu_{B1}}$, $\overline{\delta\nu_{A1}}-\overline{\delta\nu_{B1}}\approx -ER_{AB}$. Since only the ionic state Eq. (3.3) contributes to Eq. (3.23), $\delta\rho$ of Eq. (3.23) represents interatomic charge transfer from the up-field atom H_B to the down-field H_A, which in the minimal orbital model vanishes with R(H–H) proportionally to S_1^2. Evidently, the minimal orbital model does not recover the true limit for dissociating H_2, which would be a nonzero (though small) $\delta\rho$, representing interaatomic polarization of noninteracting H atoms. The proper description can be achieved only with an extended orbital model which, besides $1s$ AOs, employs also $2s$,$2p$ AOs. The extended model will be considered in Sec. V.

IV. AN ASYMPTOTIC CORRECTION FOR THE ALDA MATRIX ELEMENTS

From Eqs. (3.13)–(3.17) one can attempt to derive the asymptotic expressions for the matrix elements $K_{12,12}^{xc(\uparrow\uparrow)}$ and $K_{12,12}^{xc(\uparrow\downarrow)}$. The additional useful information is that the matrix element $K_{12,12}^{xc(\uparrow\uparrow)}$ for electrons with the same spin can be further subdivided in exchange and correlation parts, $K_{12,12}^{xc(\uparrow\uparrow)}=K_{12,12}^{x(\uparrow\uparrow)}+K_{12,12}^{c(\uparrow\uparrow)}$ and the exchange part in the case of the two-electron closed-shell H_2 is just minus the Coulomb integral

$$K_{12,12}^{x(\uparrow\uparrow)}=-K_{12,12}^{Coul}, \tag{4.1}$$

which provides the exclusion of the electron self-interaction. Based on Eqs. (3.13)–(3.17) and (4.1), we propose the following asymptotic expression for both matrix elements $K_{12,12}^{xc(\uparrow\uparrow)}$ and $K_{12,12}^{xc(\uparrow\downarrow)}$:

$$K_{12,12}^{xc(\uparrow\uparrow)(asymp)}=K_{12,12}^{xc(\uparrow\downarrow)(asymp)}=\frac{(K_{12,12}^{Coul})^2}{\Delta\varepsilon_{21}}-K_{12,12}^{Coul}. \tag{4.2}$$

Inserting Eq. (4.2) in (3.13), one can see that the finite integrals $K_{12,12}^{Coul}$ in the Coulomb, exchange, and correlation parts cancel each other. Thus, neglecting a small $\Delta\varepsilon_{21}^2$ term, we obtain for the singlet excitation ω_{s1}

$$\omega_{s1}\sim 2K_{12,12}^{Coul}, \tag{4.3}$$

which is a fair asymptotic estimate for the energy of excitation from the covalent configuration to the ionic configuration. On the other hand, the components $K_{12,12}^{xc(\uparrow\uparrow)(asymp)}$ and $K_{12,12}^{xc(\uparrow\downarrow)(asymp)}$ cancel each other in the expression Eq. (3.14) for the triplet excitation ω_{t1}, so that we obtain the proper zero asymptotics for ω_{t1}.

The expression Eq. (4.2) incorporates the asymptotic divergence of the xc matrix elements, which has been established with the analysis of the eigenvalue problem. It can be used to correct the ALDA matrix elements $K_{12,12}^{xc(\uparrow\uparrow)(ALDA)}$ and $K_{12,12}^{xc(\uparrow\downarrow)(ALDA)}$ calculated with the ALDA xc kernel Eq. (1.8). Since ALDA yields a reasonable estimate of the excitation energies ω_{s1} and ω_{t1} for shorter R(H–H) where the HOMO-LUMO gap $\Delta\varepsilon_{21}$ is relatively large, but fails at larger R(H–H) where $\Delta\varepsilon_{21}$ is small, one can use $\Delta\varepsilon_{21}$ as an argument for exponential interpolation between $K_{12,12}^{xc(ALDA)}$ and $K_{12,12}^{xc(asymp)}$ in order to produce corrected elements $\tilde{K}_{12,12}^{xc}$:

$$\tilde{K}_{12,12}^{xc(\uparrow\uparrow)}=[1-\exp(-k[\Delta\varepsilon_{21}]^2)]K_{12,12}^{xc(\uparrow\uparrow)(ALDA)} +\exp(-k[\Delta\varepsilon_{21}]^2)K_{12,12}^{xc(\uparrow\uparrow)(asymp)}, \tag{4.4}$$

$$\tilde{K}_{12,12}^{xc(\uparrow\downarrow)}=[1-\exp(-k[\Delta\varepsilon_{21}]^2)]K_{12,12}^{xc(\uparrow\downarrow)(ALDA)} +\exp(-k[\Delta\varepsilon_{21}]^2)K_{12,12}^{xc(\uparrow\downarrow)(asymp)}. \tag{4.5}$$

At the equilibrium geometry, the dominant terms of Eqs. (4.4) and (4.5) will be the ALDA ones, while for larger R(H–H) the decrease of $\Delta\varepsilon_{21}$ will lead to larger contributions from $K_{12,12}^{xc(\uparrow\uparrow)(asymp)}$ and $K_{12,12}^{xc(\uparrow\downarrow)(asymp)}$, thus providing a proper behavior of the corrected matrix elements.

We proceed with calculations for the dissociating H_2 with the asymptotically corrected ALDA (ALDA-AC) of Eqs. (4.4), (4.5); see Fig. 3. The important point is that in the eigenvalue Eqs. (3.5)–(3.9) the corrections are added only to the diagonal matrix elements $K_{12,12}^{xc}$ between the HOMOψ_1 and LUMOψ_2. They are not added to other diagonal or off-diagonal elements; in particular, they are not added to the coupling elements $K_{1c,1c}^{xc}$ between ψ_1 and unoccupied orbitals ψ_c, which consist of $2s$ and $2p$ AOs (the calculations displayed in Fig. 3 have been carried out with the extended orbital model). Thus we use the elements $\tilde{K}_{12,12}^{xc(\uparrow\uparrow)}$ and $\tilde{K}_{12,12}^{xc(\uparrow\downarrow)}$ of Eqs. (4.4), (4.5) for the coupling between ψ_1 and ψ_2,

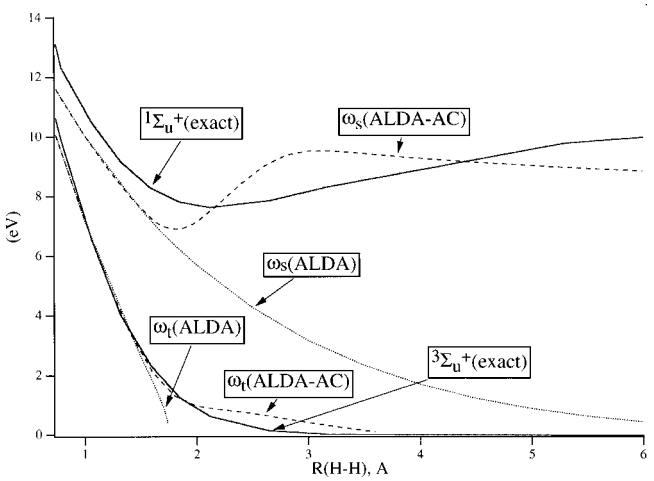

FIG. 3. Comparison of the exact and ALDA-AC and ALDA differential potential curves for H_2.

while for other couplings the elements $K_{ic,Jd}^{\mathrm{xc(ALDA)}}$ of the standard ALDA are retained. No explicit frequency dependence of the matrix elements is introduced and we remain, formally, in the domain of the adiabatic approximation. In this context, the use of different expressions for the matrix elements of different orbitals simply means that we are trying to reproduce properly the action of a spatially nonlocal xc kernel $f_{\mathrm{xc}}(\mathbf{r},\mathbf{r}')$ on those orbitals. It will be argued in the next section that the use of different expressions for the matrix elements of different orbitals simulates a rather complex spatial behavior of the xc kernel $f_{\mathrm{xc}}(\mathbf{r},\mathbf{r}',\omega)$ with diverging behavior only in the atomic regions.

Figure 3 compares the exact differential potential curves with those calculated with the ALDA and ALDA-AC with the parameter $k=100$. The functions Eqs. (4.4), (4.5) radically improve the performance of TDDFPT for the singlet excitation. Unlike the purely repulsive ALDA curve (see Fig. 1), the ALDA-AC curve exhibits a minimum, although it is somewhat displaced from that of the exact curve. The ALDA-AC curve does not depart very far from the exact one and the calculated excitation energy does not vanish with R(H–H) as was the case for the standard ALDA. The ALDA-AC potential energy curve does not go asymptotically to an ionic H^+-H^- situation, but in agreement with the exact curve it exhibits the effect of the avoided crossing at larger distance of the ionic $\psi_1\rightarrow\psi_2$ $^1\Sigma_u^+$ excited state [Ψ_2^{HL}, Eq. (3.3)] by a $^1\Sigma_u^+$ state representing a H–H* system i.e., one H atom is excited. The excitation will be to $2s$ with admixture of a $1s\rightarrow 2p_\sigma$ excited state. So in the TDDFT calculation the $^1\Sigma_u^+$ excitation energy asymptotically no longer corresponds to a pure transition from the HOMOψ_1 of Eq. (2.1) to the LUMOψ_2 of Eq. (2.2). Starting from R(H–H)$\approx$2.50 Å, as indicated by the analysis of the calculated weights of the single-particle transitions, an appreciable contribution comes from the transition from the HOMO to the antibonding orbital ψ_3

$$\psi_3(\mathbf{r})=2\sigma_u(\mathbf{r})=\frac{1}{\sqrt{2-2S}}[a^{\mathrm{hyb}}(\mathbf{r})-b^{\mathrm{hyb}}(\mathbf{r})], \qquad (4.6)$$

where $a^{\mathrm{hyb}}(\mathbf{r})$ and $b^{\mathrm{hyb}}(\mathbf{r})$ are hybrid orbitals consisting of $2s,2p_\sigma$ AOs of atoms H_A and H_B, respectively. At R(H–H)=3.0 Å the transitions $\psi_1\rightarrow\psi_2$ and $\psi_1\rightarrow\psi_3$ bring almost equal contributions; at larger R(H–H) the contribution of the former transition gradually vanishes, and for R(H–H)$\geqslant$4.0 Å the lowest singlet transition becomes an almost pure $\psi_1\rightarrow\psi_3$ transition. As a result, the singlet excitation energy calculated by ALDA-AC approaches the value $\Delta\varepsilon_{31}=8.6$ eV, which is just the LDA difference between the energies of the orbitals ψ_1 and ψ_3. In fact, some oscillation of the ALDA-AC singlet curve around the exact one appears to occur just because of the difference of the corresponding asymptotics, 10.2 eV for the exact curve, corresponding to the exact $1s\rightarrow 2s$ excitation, and 8.6 eV for the TDDFT curve, corresponding to the LDA$1s$-$2s$ orbital energy difference. The asymptotic error of ALDA-AC is an artifact of the ground state LDA calculations with the xc potential $\nu_{\mathrm{xc}}^{(\mathrm{LDA})}$. The exact KS potential of dissociated H_2 will have to produce the exact H atom density around each H nucleus, i.e., the occupied orbital ψ_1 must in that region be identical to the H $1s$ atomic orbital and the KS potential must be equal to the bare nuclear potential of the H atom. The unoccupied KS $2s$ orbital must also have the exact $2s$ orbital energy and a TDDFT calculation based on an exact KS potential should provide an exact value $\Delta\varepsilon_{31}=10.2$ eV, which is the atomic energy of $1s\rightarrow 2s$ or $2p$ promotion. Thus further improvement of the TDDFPT results can be achieved by the replacement of $\nu_{\mathrm{xc}}^{(\mathrm{LDA})}$ with a more refined potential, which would incorporate correctly the effects of exchange and nondynamical correlation in dissociating H_2 so as to produce the bare nuclear field around each H atom. The corresponding refinement still presents a problem for DFT and, to the best of our knowledge, none of the existing model potentials can guarantee the proper dissociation limit. It is interesting to observe that singly excited configuration $\psi_1\psi_3=1\sigma_g 2\sigma_u$, although capable of yielding in the TDDFT calculation an exact excitation energy, does not correspond to a correct asymptotic wave function. Completely analogous to the situation for the ground state, where the determinant $|1\sigma_g\alpha 1\sigma_g\beta|$ is an equal mixture of ionic and covalent wave functions, the configuration $1\sigma_g 2\sigma_u$ leads to an equal mixture of ionic configurations, describing negative H^- ions with an electron in $1s$ and a promoted electron in $2s$, and ''covalent'' configurations with a $1s$ electron on one H and a promoted electron in $2s$ on the other H. To get a correct wave function without ionic character one needs configuration mixing with the *doubly excited* configuration $1\sigma_u 2\sigma_g$ to remove the ionic terms. We have here a case where the solution vector **F** of the eigenvalue problem Eq. (3.5) or (3.6), which has only coefficients referring to singly excited configurations, does not at all represent the composition of the excited state wave function. This is related with the fact that the ground state KS determinant in this case is not a good approximation of the ground state wave function, for which admixture of the doubly excited configuration $(1\sigma_u)^2$ is needed.

The function Eqs. (4.4), (4.5) also definitely improves the performance of TDDFPT for the triplet excitation (see Fig. 3). The ALDA-AC curve goes closer to the exact one in a larger interval than the ALDA curve. Due to the admixture of the LDA functional in Eqs. (4.4), (4.5) the ALDA-AC

curve also suffers from the triplet instability, although the corresponding instability point at $R(\mathrm{H–H})=3.6$ Å is about twice as far out as the ALDA instability point at 1.75 Å. Further refinement of the simple model Eq. (4.4), (4.5) will, hopefully, remove the triplet instability altogether.

V. RESPONSE FUNCTION χ AND FIELD-COUNTERACTING TERM OF THE xc POTENTIAL IN THE EXTENDED $1s,2s,2p$ MODEL

Our discussion of the behavior of f_{xc} and the asymptotic behavior of the $K_{12,12}$ matrix elements has employed the minimal orbital model for H_2. The conclusions should not be dependent on the use of this limited model, and in this section we shall consider an extension of the minimal two-orbital model of Sec. III. In this $1s,2s,2p$ model the set Eqs. (3.1)–(3.4) of the Heitler–London wave functions of the minimal model is extended with additional HL functions, which describe $1s\rightarrow 2s,2p$ electron promotions. We will derive the response function $\chi(\mathbf{r},\mathbf{r}',\omega)$ within this extended model, and the KS response function $\chi_s(\mathbf{r},\mathbf{r}',\omega)$. As expected, the polarizability derived with $\chi(\mathbf{r},\mathbf{r}',\omega)$ will now correctly reproduce the intra-atomic polarizations of the dissociating H atoms. We will also derive from the response functions the established occurrence of a counteracting field[40] in the KS potential for stretched H_2 in a external field,[30,41] or in $\delta\nu_{\mathrm{xc}}$ in linear response calculations. In particular, however, this section will serve to study the asymptotic behavior of f_{xc} beyond the rather limited minimal orbital model.

Only $^1\Sigma$ states are considered, since these are important for our further analysis. They are represented with the following functions:

$$\Psi_4^{HL}(^1\Sigma_u^+)=\frac{1}{2^{3/2}(1-S_1S_2+S_{12}^2)^{1/2}}[a_1(\mathbf{r}_1)b_2(\mathbf{r}_2)-b_1(\mathbf{r}_1)a_2(\mathbf{r}_2)+a_1(\mathbf{r}_2)b_2(\mathbf{r}_1)-b_1(\mathbf{r}_2)a_2(\mathbf{r}_1)][\alpha(1)\beta(2)-\beta(1)\alpha(2)], \tag{5.1}$$

$$\Psi_5^{HL}(^1\Sigma_u^+)=\frac{1}{2^{3/2}(1-S_1S_3+S_{13}^2)^{1/2}}[a_1(\mathbf{r}_1)b_3(\mathbf{r}_2)-b_1(\mathbf{r}_1)a_3(\mathbf{r}_2)+a_1(\mathbf{r}_2)b_3(\mathbf{r}_1)-b_1(\mathbf{r}_2)a_3(\mathbf{r}_1)][\alpha(1)\beta(2)-\beta(1)\alpha(2)], \tag{5.2}$$

$$\Psi_6^{HL}(^1\Sigma_g^+)=\frac{1}{2^{3/2}(1+S_1S_2+S_{12}^2)^{1/2}}[a_1(\mathbf{r}_1)b_2(\mathbf{r}_2)+b_1(\mathbf{r}_1)a_2(\mathbf{r}_2)+a_1(\mathbf{r}_2)b_2(\mathbf{r}_1)+b_1(\mathbf{r}_2)a_2(\mathbf{r}_1)][\alpha(1)\beta(2)-\beta(1)\alpha(2)], \tag{5.3}$$

$$\Psi_7^{HL}(^1\Sigma_g^+)=\frac{1}{2^{3/2}(1+S_1S_3+S_{13}^2)^{1/2}}[a_1(\mathbf{r}_1)b_3(\mathbf{r}_2)+b_1(\mathbf{r}_1)a_3(\mathbf{r}_2)+a_1(\mathbf{r}_2)b_3(\mathbf{r}_1)+b_1(\mathbf{r}_2)a_3(\mathbf{r}_1)][\alpha(1)\beta(2)-\beta(1)\alpha(2)], \tag{5.4}$$

where $a_2(\mathbf{r}),b_2(\mathbf{r})$ are $2s$ AOs and $a_3(\mathbf{r}),b_3(\mathbf{r})$ are $2p_\sigma$ AOs located on atoms H_A and H_B, respectively, S_2 is the overlap integral between $a_2(\mathbf{r})$ and $b_2(\mathbf{r}),S_3$ is that between $a_3(\mathbf{r})$ and $b_3(\mathbf{r}),S_{12}$ is the overlap integral between $a_1(\mathbf{r})$ and $b_2(\mathbf{r})$, and S_{13} is that between $a_1(\mathbf{r})$ and $b_3(\mathbf{r})$.

The interacting response function χ calculated in this model has terms arising from the functions Eqs. (5.1)–(5.4) in addition to those of Eq. (3.21)

$$\chi(\mathbf{r},\mathbf{r}',\omega)=\sum_{j=2}^{7}\frac{2[E_j-E_0]}{\omega^2-[E_j-E_0]^2}\langle\Psi_0^{HL}|\hat{\rho}(\mathbf{r})|\Psi_j^{HL}\rangle\langle\Psi_j^{HL}|\hat{\rho}(\mathbf{r}')|\Psi_0^{HL}\rangle$$

$$=\frac{2(E_2-E_0)}{[\omega^2-(E_2-E_0)^2]}\frac{S_1^2}{(1-S_1^2)^2}[a_1^2(\mathbf{r})-b_1^2(\mathbf{r})][a_1^2(\mathbf{r}')-b_1^2(\mathbf{r}')]+\frac{2(E_3-E_0)}{[\omega^2-(E_3-E_0)^2]}$$

$$\times\frac{[-S_1a_1^2(\mathbf{r})-S_1b_1^2(\mathbf{r})+2a_1(\mathbf{r})b_1(\mathbf{r})]}{(1+S_1^2)}\frac{[-S_1a_1^2(\mathbf{r}')-S_1b_1^2(\mathbf{r}')+2a_1(\mathbf{r}')b_1(\mathbf{r}')]}{(1+S_1^2)}$$

$$+\sum_{i=2}^{3}\frac{(E_{i+2}-E_0)}{[\omega^2-(E_{i+2}-E_0)^2]}\frac{1}{(1+S_1^2)^{1/2}(1-S_1S_i+S_{1i}^2)}$$

$$\times[a_1(\mathbf{r})a_i(\mathbf{r})-b_1(\mathbf{r})b_i(\mathbf{r})+S_1b_1(\mathbf{r})a_i(\mathbf{r})-S_1a_1(\mathbf{r})b_i(\mathbf{r})][a_1(\mathbf{r}')a_i(\mathbf{r}')-b_1(\mathbf{r}')b_i(\mathbf{r}')$$

$$+S_1b_1(\mathbf{r}')a_i(\mathbf{r}')-S_1a_1(\mathbf{r}')b_i(r')]+\sum_{i=2}^{3}\frac{(E_{i+4}-E_0)}{[\omega^2-(E_{i+4}-E_0)^2]}\frac{1}{(1+S_1^2)^{1/2}(1+S_1S_i+S_{1i}^2)}$$
$$\times[a_1(\mathbf{r})a_i(\mathbf{r})+b_1(\mathbf{r})b_i(\mathbf{r})+S_1b_1(\mathbf{r})a_i(\mathbf{r})+S_1a_1(\mathbf{r})b_i(\mathbf{r})+2S_{1i}a_1(\mathbf{r})b_1(\mathbf{r})]$$
$$\times[a_1(\mathbf{r}')a_i(\mathbf{r}')+b_1(\mathbf{r}')b_i(\mathbf{r}')+S_1b_1(\mathbf{r}')a_i(\mathbf{r}')+S_1a_1(\mathbf{r}')b_i(\mathbf{r}')+2S_{1i}a_1(\mathbf{r}')b_1(\mathbf{r}')]. \quad (5.5)$$

Unlike the function Eq. (3.21) of the minimal model, the response function Eq. (5. 5) of the extended model contains in the numerators of the last two sums the one-center terms $a_1(\mathbf{r})a_i(\mathbf{r})$ and $b_1(\mathbf{r})b_i(\mathbf{r})$, which represents $1s\rightarrow 2s,2p$ promotions, and do not vanish with R(H–H). Then, neglecting all the terms with overlap integrals in Eq. (5.5), one can obtain the following asymptotic expression of $\chi(\omega)$ for all frequencies except those in the neighborhood of the resonance frequencies:

$$\chi(\mathbf{r},\mathbf{r}',\omega)\approx\sum_{i=2}^{3}\frac{(E_{i+2}-E_0)}{[\omega^2-(E_{i+2}-E_0)^2]}[a_1(\mathbf{r})a_i(\mathbf{r})-b_1(\mathbf{r})b_i(\mathbf{r})][a_1(\mathbf{r}')a_i(\mathbf{r}')-b_1(\mathbf{r}')b_i(\mathbf{r}')]$$
$$+\sum_{i=2}^{3}\frac{(E_{i+4}-E_0)}{[\omega^2-(E_{i+4}-E_0)^2]}\times[a_1(\mathbf{r})a_i(\mathbf{r})+b_1(\mathbf{r})b_i(\mathbf{r})][a_1(\mathbf{r}')a_i(\mathbf{r}')+b_1(\mathbf{r}')b_i(\mathbf{r}')]. \quad (5.6)$$

So $\chi(\omega)$ does not any more go to zero like S_1^2, but as one can see from Eq. (5.6) that the function $\chi(\omega)$ will have nonzero values in large $\mathbf{r}$ and $\mathbf{r}'$ regions for R(H–H)$\rightarrow\infty$ (in particular, also in the static limit $\omega\rightarrow 0$). From the finiteness of $\chi(\mathbf{r},\mathbf{r}',\omega)$ of Eq. (5.6) it follows that we can no longer conclude that the inverse response function $\chi^{-1}(\mathbf{r},\mathbf{r}',\omega)$ has to diverge.

The noninteracting response function χ_s can be written in the extended model as follows:

$$\chi_s(\mathbf{r},\mathbf{r}',\omega)=\frac{4\Delta\varepsilon_{21}}{\omega^2-\Delta\varepsilon_{21}^2}\psi_1(\mathbf{r})\psi_2(\mathbf{r})\psi_2(\mathbf{r}')\psi_1(\mathbf{r}')+\sum_{c=3}^{6}\frac{4\Delta\varepsilon_{c1}}{\omega^2-\Delta\varepsilon_{c1}^2}\psi_1(\mathbf{r})\psi_c(\mathbf{r})\psi_c(\mathbf{r}')\psi_1(\mathbf{r}'), \quad (5.7)$$

where $\psi_3-\psi_6$ are the bonding and antibonding KS orbitals built from $2s,2p_\sigma$ AOs and $\Delta\varepsilon_{c1}$ are the corresponding energy differences $\Delta\varepsilon_{c1}=\varepsilon_c-\varepsilon_1$. Just as the function Eq. (3.19) of the minimal model, $\chi_s(\omega)$ of Eq. (5.7) diverges as $-(\Delta\varepsilon_{21})^{-1}$ at small frequencies $|\omega|<\Delta\varepsilon_{21}$. However, unlike Eq. (3.19), $\chi_s(\omega)$ of Eq. (5.7) is finite at larger frequencies $|\omega|>\Delta\varepsilon_{21}$, since its first term vanishes, while other terms are finite due to the finiteness of the energy differences $\Delta\varepsilon_{c1}$. From this follows, that the inverse response function $\chi_s^{-1}(\mathbf{r},\mathbf{r}',\omega)$ vanishes at $|\omega|<\Delta\varepsilon_{21}$ and it remains finite at $|\omega|>\Delta\varepsilon_{21}$.

We now first consider the static density response $\delta\rho(\mathbf{r},0)$ to an external field $\delta\nu_{\mathrm{ex}}(\mathbf{r})=Ez$ as obtained from the interacting response function $\chi(\mathbf{r},\mathbf{r}',\omega)$. In fact, the intraatomic polarization terms, which are lacking in the expression Eq. (3.23) of the minimal model, are properly introduced by the $\chi(\mathbf{r},\mathbf{r}',\omega)$ of the extended model. To see this, one can insert the expression Eq. (5.6) into the formula Eq. (3.22). The second sum of Eq. (5.6) has zero contribution to $\delta\rho$ due to the symmetry, which yields the following asymptotic expression for $\delta\rho(\mathbf{r},0)$

$$\delta\rho(\mathbf{r},0)=\frac{[\delta\overline{\nu}_{B2}-\delta\overline{\nu}_{A2}]}{(E_4-E_0)}[a_1(\mathbf{r})a_2(\mathbf{r})-b_1(\mathbf{r})b_2(\mathbf{r})]+\frac{[\delta\overline{\nu}_{B3}-\delta\overline{\nu}_{A3}]}{(E_5-E_0)}[a_1(\mathbf{r})a_3(\mathbf{r})-b_1(\mathbf{r})b_3(\mathbf{r})], \quad (5.8)$$

where $\delta\overline{\nu}_{Ai}$ and $\delta\overline{\nu}_{Bi}$ are the one-center field integrals $\delta\overline{\nu}_{Ai}=\int d\mathbf{r}a_1(\mathbf{r})\delta\nu_{\mathrm{ext}}(\mathbf{r})a_i(\mathbf{r})$, $\delta\overline{\nu}_{Bi}=\int d\mathbf{r}b_1(\mathbf{r})\delta\nu_{\mathrm{ext}}(\mathbf{r})b_i(\mathbf{r})$. Unlike the vanishing density response Eq. (3.23) of the minimal model, $\delta\rho(\mathbf{r},0)$ of Eq. (5.8) remains finite at R(H–H) $\rightarrow\infty$. It represents the correct intraatomic polarization of noninteracting H atoms. Indeed, while the orbital products $b_1^2(\mathbf{r})$ and $a_1^2(\mathbf{r})$ in Eq. (3.23) are both positive and, taken together, produce interatomic charge transfer, each of the products $a_1(\mathbf{r})a_i(\mathbf{r})$ and $b_1(\mathbf{r})b_i(\mathbf{r})$ in Eq. (5.8) changes sign inside the corresponding atom and they produce intraatomic polarization. In particular, the first term of Eq. (5.8) represents ''in–out'' polarization from $1s$ to $2s$ AOs, while the second term represents ''left–right'' polarization from $1s$ to $2p_\sigma$ AOs and the signs of the products $a_1(\mathbf{r})a_3(\mathbf{r})$ and $b_1(\mathbf{r})b_3(\mathbf{r})$ provide the proper polarization of the density along the field.

With the response Eq. (5.8), the change of the xc potential can be expressed as the following integral with the xc kernel:

$$\delta\nu_{\mathrm{xc}}(\mathbf{r})=\int d\mathbf{r}'\,\delta\rho(\mathbf{r}')f_{\mathrm{xc}}(\mathbf{r},\mathbf{r}')=\frac{[\delta\overline{\nu}_{B2}-\delta\overline{\nu}_{A2}]}{(E_4-E_0)}\int d\mathbf{r}'[a_1(\mathbf{r}')a_2(\mathbf{r}')-b_1(\mathbf{r}')b_2(\mathbf{r}')]f_{\mathrm{xc}}(\mathbf{r},\mathbf{r}')$$
$$+\frac{[\delta\overline{\nu}_{B3}-\delta\overline{\nu}_{A3}]}{(E_5-E_0)}\int d\mathbf{r}'[a_1(\mathbf{r}')a_3(\mathbf{r}')-b_1(\mathbf{r}')b_3(\mathbf{r}')]f_{\mathrm{xc}}(\mathbf{r},\mathbf{r}'). \quad (5.9)$$

The potential $\delta\nu_{\mathrm{xc}}(\mathbf{r})$ is a part of the KS response expression Eq. (1.3) in the special case of $\omega=0$

$$\delta\rho(\mathbf{r}) = \int d\mathbf{r}'\chi_s(\mathbf{r},\mathbf{r}') \times \left\{ \delta\nu_{\mathrm{ext}}(\mathbf{r}') + \int d\mathbf{r}'' \frac{\delta\rho(\mathbf{r}'')}{|\mathbf{r}'-\mathbf{r}''|} + \delta\nu_{\mathrm{xc}}(\mathbf{r}') \right\}. \tag{5.10}$$

Note, that $\delta\rho(\mathbf{r})$ in the l.h.s. of Eq. (5.10) is, of course, the well-defined and finite function Eq. (5.8). However, as follows from Eq. (5.7) that the static KS response function $\chi_s(\mathbf{r},\mathbf{r}')$ diverges as $(\Delta\varepsilon_{21})^{-1}$ with R(H–H). From this it follows that the potential changes within the brackets of Eq. (5.10) should cancel each other:

$$\delta\nu_{\mathrm{xc}}(\mathbf{r}') \approx -\delta\nu_{\mathrm{ext}}(\mathbf{r}') - \int d\mathbf{r}'' \frac{\delta\rho(\mathbf{r}'')}{|\mathbf{r}'-\mathbf{r}''|}. \tag{5.11}$$

Thus with Eq. (5.11) TDDFPT requires generation of a field-counteracting term $\delta\nu_{\mathrm{xc}}$ in the xc potential, which compensates the combined effect of the external field and the induced Hartree potential in order to produce with $\chi_s(\mathbf{r},\mathbf{r}')$ a finite density response Eq. (5.8). This compensation means that the potential change $\delta\nu_{\mathrm{xc}}(\mathbf{r})$ should be positive on the low-field atom H_A and it should be negative on the high-field atom H_B. This is $-\delta\nu_{\mathrm{ext}}$. Since $\delta\rho$ only represents polarization of atomic density, its potential is basically zero (no monopole term) and indeed

$$\delta\nu_{\mathrm{xc}}(\mathbf{r}) \approx -\delta\nu_{\mathrm{ext}}(\mathbf{r}). \tag{5.12}$$

Thus a field-counteracting term emerges in the xc potential, which completely compensates the external field in the dissociation limit. Note that such a term is lacking in LDA and GGAs, which is related to the established failure of the ALDA for the excitation energies.

Finally we address the question what one can conclude about f_{xc} and its matrix elements $K^{\mathrm{xc}}_{ic,jd}$ in the extended model. We have observed that the divergence of $\chi^{-1}(\omega)$ at all frequencies and the divergence of $\chi_s^{-1}(\omega)$ at $\omega \gg \Delta\varepsilon_{21}$ found in the minimal model will not apply strictly in the extended model. Indeed, while the first two terms of Eq. (5.5) vanish with R(H–H), the additional terms contain in the numerators the one-center orbital products $a_1(\mathbf{r})a_i(\mathbf{r})$ and $b_1(\mathbf{r})b_i(\mathbf{r})$, which represent $1s \rightarrow 2s,2p$ promotions, and do not vanish with R(H–H). Note that these two groups of terms are located in different regions. Containing the orbital products ${a_1}^2(\mathbf{r})$ and $b_1^2(\mathbf{r})$, the vanishing terms are localized in atomic regions, while the products $a_1(\mathbf{r})a_i(\mathbf{r})$ and $b_1(\mathbf{r})b_i(\mathbf{r})$ with the diffuse orbitals $a_i(\mathbf{r})$ and $b_i(\mathbf{r})$ bring the nonvanishing terms to the outer regions of the atomic periphery. Thus one can come to the conclusion, that the interacting response function Eq. (5.5) of the extended model becomes very small only in the atomic regions, while it remains finite at the atomic periphery. From this picture for $\chi(\mathbf{r},\mathbf{r}',\omega)$ one can expect that the corresponding inverse response function $\chi^{-1}(\mathbf{r},\mathbf{r}',\omega)$ diverges in the atomic regions, while it remains finite at the atomic periphery.

For the noninteracting response function χ_s, Eq. (5.7), we have a picture similar to that for the interacting function Eq. (5.5): the first term of Eq. (5.7) is localized in the atomic regions, while other terms are localized in the outer regions. Then, the first term diverges as $-(\Delta\varepsilon_{21})^{-1}$ at small frequencies $|\omega| < \Delta\varepsilon_{21}$ and it vanishes as $\Delta\varepsilon_{21}$ at larger frequencies $|\omega| > \Delta\varepsilon_{21}$, while other terms of Eq. (5.7) remain finite. Thus at $|\omega| > \Delta\varepsilon_{21}$ the noninteracting response function $\chi_s(\mathbf{r},\mathbf{r}',\omega)$ vanishes in the atomic regions and it is finite in the outer regions. One can expect, that the corresponding inverse function $\chi_s^{-1}(\mathbf{r},\mathbf{r}',\omega)$ diverges in the atomic regions, and is finite at the atomic periphery.

From these results and the relation Eq. (3.18) one can conclude that the extended model leads to a complex spatial structure of the xc kernel $f_{\mathrm{xc}}(\mathbf{r},\mathbf{r}',\omega)$ with diverging behavior only in certain regions. $f_{\mathrm{xc}}(\mathbf{r},\mathbf{r}',\omega)$ diverges in the atomic regions, where $\chi^{-1}(\mathbf{r},\mathbf{r}',\omega)$ diverges, while $\chi_s^{-1}(\mathbf{r},\mathbf{r}',\omega)$ vanishes at $|\omega| < \Delta\varepsilon_{21}$ and diverges at $|\omega| > \Delta\varepsilon_{21}$. On the other hand, $f_{\mathrm{xc}}(\mathbf{r},\mathbf{r}',\omega)$ remains finite at the atomic periphery, where both $\chi(\mathbf{r},\mathbf{r}',\omega)$ and $\chi_s^{-1}(\mathbf{r},\mathbf{r}',\omega)$ are finite. This conclusion of the extended model generalizes that of the minimal model in Sec. III. The established complex spatial behavior of f_{xc} could be, in principle, reproduced in some analytical form, although the corresponding expression for $f_{\mathrm{xc}}(\mathbf{r},\mathbf{r}')$ might be rather involved. For TDDFPT applications, however, only matrix elements $K^{\mathrm{xc}}_{ic,jd}$ of $f_{\mathrm{xc}}(\mathbf{r},\mathbf{r}')$ are required, and the present corrections Eqs. (4.4) and (4.5) simulate the effect of the complex spatial structure of $f_{\mathrm{xc}}(\mathbf{r},\mathbf{r}')$ on $K^{\mathrm{xc}}_{ic,jd}$. Indeed, the introduced divergence of the matrix elements $K^{\mathrm{xc}}_{12\sigma,12\tau}$ corresponds to these integrals involving spatial integrations with the $1s$ functions $a_1^2(\mathbf{r})$ and $b_1^2(\mathbf{r})$ as ''weighting'' functions. These integrations therefore sample f_{xc} in the atomic region where it has diverging behavior. On the other hand, the finiteness of the matrix elements $K^{\mathrm{xc}}_{13\sigma,13\tau}$ corresponds to the finiteness of $f_{\mathrm{xc}}(r,r')$ at the atomic periphery, where the products $a_1(\mathbf{r})a_i(\mathbf{r})$ and $b_1(\mathbf{r})b_i(\mathbf{r})$ have significant values.

VI. CONCLUSIONS

In this paper time-dependent density functional perturbation theory (TDDFPT) has been applied to calculation of the differential potential curves of the lowest excited ${}^3\Sigma_u^+$ and ${}^1\Sigma_u^+$ states of H_2. It has been found that the standard TDDFPT method ALDA fails to reproduce the correct form of both potential curves. The ALDA curve for the ${}^3\Sigma_u^+$ state displays the triplet instability of the ALDA solution, while the ALDA curve for the ${}^1\Sigma_u^+$ state, instead of having the correct positive asymptotics, approaches the zero asymptotics at larger R(H–H).

The main conclusion of this paper is that ALDA fails due to a breakdown of its simple spatially local approximation for the xc kernel $f_{\mathrm{xc}}(\mathbf{r},\mathbf{r}',\omega)$ in the case of dissociating H_2. The combined analysis of the eigenvalue problem for the excitation energies and the direct estimate of the xc kernel has indicated a complex structure of the function $f_{\mathrm{xc}}(\mathbf{r},\mathbf{r}',\omega)$, which is revealed in a different behavior of the corresponding matrix elements $K^{\mathrm{xc}}_{1c,1c}$ with the bond distance R(H–H). In particular, the matrix element $K^{\mathrm{xc}}_{12,12}$ for the orbital ψ_2, which represents the ionic configuration, has been found to diverge with R(H–H), while the matrix elements for the orbitals ψ_c, which represent an electron promoted to $2s$ and $2p$ AOs, are to be finite. The complex structure of

$f_{xc}(\mathbf{r},\mathbf{r}',\omega)$ that could lead to this behavior of the matrix elements has been estimated from the extended Heitler–London model with $1s,2s,2p$ AOs, which showed possible divergence of $f_{xc}(\mathbf{r},\mathbf{r}',\omega)$ in atomic regions, while it will remain finite in the atomic periphery. This spatial behavior of f_{xc} could hopefully be modeled within the adiabatic approximation with a proper function $f_{xc}(\mathbf{r},\mathbf{r}')$.

In this paper the effect of spatial nonlocality of $f_{xc}(\mathbf{r},\mathbf{r}')$ has been modeled by using different expressions for the corresponding matrix elements of different orbitals. Specifically, the asymptotically corrected ALDA (ALDA-AC) expressions Eqs. (4.4), (4.5) have been used for the matrix elements $K_{12,12}^{xc(\sigma\tau)}$, while for other matrix elements the standard ALDA expressions have been retained. This approach provides substantial improvement over the standard ALDA. In particular, the ALDA-AC curve for the lowest singlet excitation reproduces qualitative features of the exact curve. It displays a minimum and approaches a relatively large positive energy at large R(H–H). The corresponding TDDFT solution exhibits the effect of the avoided crossing of the potential curves. ALDA-AC also produces a substantial improvement for the calculated lowest triplet excitation. Further improvement of the TDDFT results can be achieved by the improvement of the ground state KS solution and refinement of the asymptotic correction Eqs. (4.4), (4.5).

The asymptotic expression for the static density response to an external field has been obtained with the calculated interacting response function χ. In the dissociation limit it represents the correct picture of the intra-atomic polarization of noninteracting H atoms. The change of the xc potential has been evaluated and the origin of the field-counteracting term in ν_{xc} has been established within TDDFPT.

The present results can be of importance for time-dependent density functional theory of photochemical reactions, where the dissociation of the H–H bond can serve as a prototype of photodissociation of a single covalent bond. As in H_2, the TDDFT zero order energy $\Delta\varepsilon$ of certain triplet and ionic singlet excitations, which correspond to the breaking of the bond, will vanish with the bond length. In this situation we anticipate the same failure of ALDA as for the present case of the dissociating H_2 and we hope that the asymptotic corrections of the type Eqs. (4.4), (4.5) will bring a similar substantial improvement of the results.

[1] E. K. U. Gross, J. F. Dobson, and M. Petersilka, in *Density Functional Theory*, Vol. 181, edited by R. F. Nalewajski (Springer, Berlin, 1996), pp. 81.
[2] M. E. Casida, in *Recent Developments and Applications of Modern Density Functional Theory*, edited by J. M. Seminario (Elsevier, Amsterdam, 1996).
[3] R. Bauernschmitt and R. Ahlrichs, Chem. Phys. Lett. **256**, 454 (1996).
[4] S. J. A. van Gisbergen, J. G. Snijders, and E. J. Baerends, Comput. Phys. Commun. **118**, 119 (1999).
[5] R. E. Stratman, G. E. Scuseria, and M. J. Frisch, J. Chem. Phys. **109**, 8218 (1998).
[6] A. Görling, H. H. Heinze, S. P. Ruzankin, M. Staufer, and N. Rösch, J. Chem. Phys. **110**, 2785 (1999).
[7] S. Hirata and M. Head-Gordon, Chem. Phys. Lett. **302**, 375 (1999).
[8] E. K. U. Gross and W. Kohn, Adv. Quantum Chem. **21**, 255 (1990).
[9] R. van Leeuwen, Phys. Rev. Lett. **80**, 1280 (1998).
[10] A. Görling, Int. J. Quantum Chem. **69**, 265 (1998).
[11] M. Casida, in *Recent Advances in Density Functional Methods*, Vol. 1, edited by D. P. Chong (World Scientific, Singapore, 1995).
[12] M. Petersilka, U. J. Gossmann, and E. K. U. Gross, Phys. Rev. Lett. **76**, 1212 (1996).
[13] S. J. A. van Gisbergen, F. Kootstra, P. R. T. Schipper, O. V. Gritsenko, J. G. Snijders, and E. J. Baerends, Phys. Rev. A **57**, 2556 (1998).
[14] M. E. Casida, K. C. Casida, and D. R. Salahub, Int. J. Quantum Chem. **70**, 933 (1998).
[15] D. J. Tozer and N. C. Handy, J. Chem. Phys. **109**, 10180 (1998).
[16] P. R. T. Schipper, O. V. Gritsenko, S. J. A. van Gisbergen, and E. J. Baerends, J. Chem. Phys. **112**, 1344 (2000).
[17] O. V. Gritsenko, P. R. T. Schipper, and E. J. Baerends, Chem. Phys. Lett. **302**, 199 (1999).
[18] R. Bauernschmitt, R. Ahlrichs, F. H. Hennrich, and M. K. Kappes, J. Am. Chem. Soc. **120**, 5052 (1998).
[19] S. J. A. van Gisbergen, J. G. Snijders, and E. J. Baerends, Phys. Rev. Lett. **78**, 3097 (1997).
[20] S. J. A. van Gisbergen, A. Rosa, G. Ricciardi, and E. J. Baerends, J. Chem. Phys. **111**, 2499 (1999).
[21] G. Ricciardi, A. Rosa, S. J. A. van Gisbergen, and E. J. Baerends, J. Phys. Chem. A **104**, 635 (2000).
[22] G. Ricciardi, A. Rosa, E. J. Baerends, and S. J. A. van Gisbergen (unpublished).
[23] S. J. A. van Gisbergen, J. A. Groeneveld, A. Rosa, J. G. Snijders, and E. J. Baerends, J. Phys. Chem. **103A**, 6835 (1999).
[24] A. Rosa, E. J. Baerends, S. J. A. van Gisbergen, E. van Lenthe, J. A. Groeneveld, and J. G. Snijders, J. Am. Chem. Soc. **121**, 10356 (1999).
[25] B. Champagne, E. Perpete, S. J. A. van Gisbergen, E. J. Baerends, J. G. Snijders, C. Soubra-Ghaoui, K. A. Robins, and B. Kirtman, J. Chem. Phys. **109**, 10489 (1998).
[26] B. Champagne, E. Perpete, S. J. A. van Gisbergen, E. J. Baerends, J. G. Snijders, C. Soubra-Ghaoui, K. A. Robins, and B. Kirtman, J. Chem. Phys. **110**, 11664 (1999).
[27] B. Champagne, E. A. Perpete, D. Jacquemin, S. J. A. van Gisbergen, E. J. Baerends, C. Soubra-Ghaoui, K. Robins, and B. Kirtman (unpublished).
[28] S. J. A. van Gisbergen (unpublished).
[29] K. Yabana and G. F. Bertsch, Int. J. Quantum Chem. **75**, 55 (1999).
[30] S. J. A. van Gisbergen, P. R. T. Schipper, O. V. Gritsenko, E. J. Baerends, J. G. Snijders, B. Champagne, and B. Kirtman, Phys. Rev. Lett. **83**, 694 (1999).
[31] O. Gritsenko, S. J. A. van Gisbergen, P. R. T. Schipper, and E. J. Baerends, Phys. Rev. A **62**, 012507 (2000).
[32] J. B. Krieger, Y. Li, and G. J. Iafrate, Phys. Rev. A **45**, 101 (1992).
[33] Z.-L. Cai and J. R. Reimers, J. Chem. Phys. **112**, 527 (2000).
[34] B. Champagne, V. Deguelle, and J. M. André, J. Mol. Struct.: THEOCHEM **332**, 93 (1995).
[35] A. Spielfiedel and N. C. Handy, Phys. Chem. Chem. Phys. **1**, 2401 (1999).
[36] W. Kolos and L. Wolniewicz, J. Chem. Phys. **43**, 2429 (1965).
[37] W. Kolos and L. Wolniewicz, J. Chem. Phys. **45**, 509 (1966).
[38] R. Bauernschmitt and R. Ahlrichs, J. Chem. Phys. **104**, 9047 (1996).
[39] O. V. Gritsenko and E. J. Baerends, Theor. Chem. Acc. **96**, 44 (1997).
[40] X. Gonze, P. Ghosez, and R. W. Godby, Phys. Rev. Lett. **74**, 4035 (1995).
[41] O. V. Gritsenko, S. J. A. van Gisbergen, and E. J. Baerends (unpublished).